



# Inhibition of hepatic bile salt uptake by Bulevirtide reduces atherosclerosis in *Oatp1a1*<sup>-/-</sup> *Ldlr*<sup>-/-</sup> mice

Begoña Porteiro<sup>1,2,3,‡</sup>, Reinout L. P. Roscam Abbing<sup>1,2,‡</sup>, Wietse In het Panhuis<sup>1,2,‡</sup> , Dirk R. de Waart<sup>1,2</sup>, Suzanne Duijst<sup>1,2</sup>, Isabelle Bolt<sup>1,2</sup>, Esther W. Vogels<sup>1,2</sup>, Johannes H. M. Levels<sup>4</sup>, Laura A. Bosmans<sup>5,6,7</sup> , Winnie G. Vos<sup>5,6,7</sup> , Ronald P. J. Oude Elferink<sup>1,2,8</sup>, Esther Lutgens<sup>5,6,7,9</sup>, and Stan F. J. van de Graaf<sup>1,2,8,\*</sup>

<sup>1</sup>Tytgat Institute for Liver and Intestinal Research, Amsterdam University Medical Center, University of Amsterdam, Amsterdam, The Netherlands; <sup>2</sup>Amsterdam Gastroenterology, Endocrinology and Metabolism (AGEM), Amsterdam University Medical Center, Amsterdam, The Netherlands; <sup>3</sup>CIMUS, Universidade de Santiago de Compostela-Instituto de Investigación Sanitaria, Santiago de Compostela, Spain; <sup>4</sup>Amsterdam UMC, Department of Experimental Vascular Medicine, and <sup>5</sup>Amsterdam UMC, location AMC, Department of Medical Biochemistry, University of Amsterdam, Amsterdam, The Netherlands; <sup>6</sup>Amsterdam Cardiovascular Sciences, Atherosclerosis & Ischemic Syndromes, Amsterdam, The Netherlands; <sup>7</sup>Amsterdam institute for Immunology and Infectious Diseases, Inflammatory Diseases, Amsterdam, The Netherlands; <sup>8</sup>Department of Gastroenterology and Hepatology, Amsterdam University Medical Centers, University of Amsterdam, Amsterdam, The Netherlands; and the <sup>9</sup>Department of Cardiovascular Medicine and Immunology, Mayo Clinic, Rochester, MN, USA

**Abstract** Bile salts can strongly influence energy metabolism through systemic signaling, which can be enhanced by inhibiting the hepatic bile salt transporter Na<sup>+</sup> taurocholate cotransporting polypeptide (NTCP), thereby delaying hepatic reuptake of bile salts to increase systemic bile salt levels. Bulevirtide is an NTCP inhibitor and was originally developed to prevent NTCP-mediated entry of Hepatitis B and D into hepatocytes. We previously demonstrated that NTCP inhibition lowers body weight, induces glucagon-like peptide-1 (GLP1) secretion, and lowers plasma cholesterol levels in murine obesity models. In humans, a genetic loss-of-function variant of NTCP has been associated with reduced plasma cholesterol levels. Here, we aimed to assess if Bulevirtide treatment attenuates atherosclerosis development by treating female *Ldlr*<sup>-/-</sup> mice with Bulevirtide or vehicle for 11 weeks. Since this did not result in the expected increase in plasma bile salt levels, we generated *Oatp1a1*<sup>-/-</sup> *Ldlr*<sup>-/-</sup> mice, an atherosclerosis-prone model with human-like hepatic bile salt uptake characteristics. These mice showed delayed plasma clearance of bile salts and elevated bile salt levels upon Bulevirtide treatment. At the study endpoint, Bulevirtide-treated female *Oatp1a1*<sup>-/-</sup> *Ldlr*<sup>-/-</sup> mice had reduced atherosclerotic lesion area in the aortic root that coincided with lowered plasma LDL-c levels, independent of intestinal cholesterol absorption. In conclusion, Bulevirtide, which is considered safe and is EMA-approved for the treatment of Hepatitis D, reduces atherosclerotic lesion area by reducing plasma LDL-c levels. We anticipate that its application may extend to atherosclerotic cardiovascular diseases, which warrants clinical trials.

**Supplementary key words** bile acids and salts/metabolism • dyslipidemias • LDL • liver • cholesterol

Bile salts are synthesized in the liver and secreted into bile, which is stored in the gallbladder. In the post-prandial state, bile is excreted into the intestines, after which bile salts are re-absorbed in the ileum via the apical sodium-dependent bile salt transporter (SLC10A2, or ASBT) for entry into the enterohepatic circulation and subsequent reuptake by the hepatocyte-specific Na<sup>+</sup> taurocholate cotransporting polypeptide (SLC10A1, or NTCP) (1). While bile salts are well-known for their role in dietary lipid absorption, they have increasingly received attention for their signaling effects on metabolism over the past decades. Bile salts act as signaling molecules by targeting, amongst others, the membrane-bound G protein-coupled bile acid receptor (GPBAR1, or TGR5) and the nuclear farnesoid X receptor (FXR), which are both expressed in various tissues. Synthetic activation of TGR5 and FXR has been shown to attenuate metabolic syndrome by promoting energy metabolism, including increased energy expenditure, glucose balance, and hepatic lipid turnover, and TGR5 agonism also has immunosuppressive effects (2). Unfortunately, continuously strong TGR5 and FXR stimulation faces challenges. TGR5 agonists have so far hardly been pursued in clinical trials as they caused side effects in pre-clinical studies including gallbladder enlargement (3, 4). While synthetic FXR

<sup>‡</sup>These authors contributed equally to this work.

\*For correspondence: Stan F. J. van de Graaf, [k.f.vandegraaf@amsterdamumc.nl](mailto:k.f.vandegraaf@amsterdamumc.nl).



agonists made it to clinical trials for the evaluation of treating cholestasis and metabolic dysfunction-associated steatotic liver disease (MASLD)/metabolic dysfunction-associated steatohepatitis (MASH) (formerly known as non-alcoholic fatty liver disease (NAFLD)/non-alcoholic steatohepatitis (NASH)), they were also found to cause side effects, including pruritus, and elevated plasma cholesterol levels (2). Given that high plasma cholesterol levels is a major driving force behind atherosclerosis development, which is the result of progressive accumulation of lipids and immune cells and chronic low-grade inflammation in the larger arteries, administration of synthetic FXR agonists might increase the risk of atherosclerotic cardiovascular diseases (asCVD).

These side effects may be circumvented by increasing endogenous bile salt signaling in a physiological, meal-induced pattern (2). This can be achieved through the inhibition of NTCP (5), which in humans is predominantly responsible for the hepatic uptake of conjugated bile salts (6). In mice, hepatic bile salt uptake is regulated by both NTCP and organic anion-transporting polypeptides (OATPs), of which the OATP1A1 isoform is suspected to contribute the most to hepatic bile salt uptake amongst OATP1A/1B isoforms (6). In the absence of *Oatp1a/1b* family members, inhibition of NTCP delays the plasma clearance of bile salts, thereby increasing bile salt signaling (6). NTCP can be inhibited pharmacologically with Bulevirtide, a synthetic peptide that selectively inhibits NTCP and was originally designed for the treatment of Hepatitis B and D since these viruses gain hepatic entry through this transporter. Bulevirtide has been evaluated in phase 2 and 3 clinical trials, where it was shown to be safe and effective in preventing Hepatitis B and D infection, while simultaneously increasing systemic bile salt levels, and is now EMA-approved for the treatment of Hepatitis D (7–9). We have previously shown in mice that increasing systemic bile salt levels by genetic deletion or pharmacological inhibition of NTCP using Bulevirtide protects against obesity, hepatosteatosis, and cholestasis (10, 11). In contrast to FXR agonists that elevate plasma cholesterol levels and potentially elevate asCVD risk, Bulevirtide lowers plasma cholesterol levels in mice (11). In line with the latter, a genetic loss-of-function variant of NTCP in humans has been associated with reduced plasma cholesterol levels (12) and a phase I exploratory study suggested similar reductions in Bulevirtide-treated volunteers with low-density lipoprotein (LDL)-cholesterol levels of >130 mg/dl (13). These findings suggest that inhibition of NTCP may attenuate atherosclerosis development by lowering plasma LDL-c levels. In the current study, we demonstrate a reduction in plasma cholesterol levels upon Bulevirtide treatment which translates to a modest attenuation of atherosclerosis development. Mechanistically, these effects coincided with elevated plasma bile salt levels following inhibition of hepatic bile salt uptake.

## MATERIALS AND METHODS

### Animals

Experiments were performed in accordance with the Institute for Laboratory Animal Research Guide for the Care and Use of Laboratory Animals and were approved by the National Committee for Animal Experiments of the Netherlands and by the Institutional Animal Care and Use Committee of the University of Amsterdam University Medical Center. All animal procedures were conformed to the guidelines from Directive 2010/63/EU of the European Parliament on the protection of animals used for scientific purposes.

Female *Ldlr*<sup>-/-</sup> mice were used as they are a widely-used model for hyperlipidemia and atherosclerosis development (14), in which the females develop atherosclerotic lesions more rapidly than male mice (15). Female *Ldlr*<sup>-/-</sup> (C57BL/6J background) mice were purchased from Jackson (Bar Harbor, Maine). To model human hepatic bile salt uptake, *Oatp1a1*<sup>-/-</sup> *Ldlr*<sup>-/-</sup> mice were generated as follows. Two sgRNAs were designed that target sequences in exons 2 and 3 of the *Oatp1a1* locus. Twenty-five ng of Cas9 mRNA and 10 ng of each guide (oligo sequences are displayed in Table 1) were injected into the cytoplasm of a zygote derived from a wild-type C57BL/6J female and *Ldlr*<sup>-/-</sup> C56BL/6J male. After injection, the zygotes were implanted into the oviducts of foster mice, from which the offspring were bred homozygously into *Oatp1a1*<sup>-/-</sup> *Ldlr*<sup>-/-</sup>.

Mice were housed under standard conditions in groups of 3–6 mice per cage in a 12:12 h light/dark cycle with ad libitum access to high-fat (22% w/w) high-cholesterol (0.16%) diet (Altromin C1090-45, Triple A Trading, Tiel, the Netherlands) and water unless stated otherwise. Mice were subcutaneously injected every day at Zeitgeber Time (ZT)8–10 (ie 8–10 h into the light phase) with Bulevirtide (2.5 mg/kg body weight in 25 mM sodium carbonate, pH 8.8, 50 mg/ml mannitol) or vehicle (25 mM sodium carbonate, pH 8.8, 50 mg/ml mannitol). This treatment regime is based on previous dosing studies. Body weight was monitored using a scale.

To study plasma clearance and biliary excretion of bile salts, male and female *Ldlr*<sup>-/-</sup> (n = 5) and *Oatp1a1*<sup>-/-</sup> *Ldlr*<sup>-/-</sup> mice (n = 3) (7–18 weeks of age) were injected with Bulevirtide (2.5 mg/kg body weight) at ZT4, two hours prior to anesthesia with a mix of ketamine/xylazine (120 and 10 mg/kg, respectively), following gallbladder cannulation and intravenous injection of radiolabeled bile salts at ZT6.

For the assessment of atherosclerosis development, female *Ldlr*<sup>-/-</sup> mice (n = 15–16 per group; 7 weeks of age) and a subsequent cohort of female *Oatp1a1*<sup>-/-</sup> *Ldlr*<sup>-/-</sup> mice (n = 15 per group; 8–12 weeks of age) were injected with Bulevirtide for a total duration of 10–11 weeks. The study duration was based on the atherosclerosis development of one mouse of each treatment group that was analyzed after 7 weeks of treatment. At the study endpoint, mice were fasted for 4 h and anesthetized with a mix of ketamine/xylazine (120 and 10 mg/kg, respectively) prior to blood collection by heart puncture and euthanasia by cervical dislocation at ZT6.

TABLE 1. *mOatp1a1* oligo's for sgRNA

Exon 2	5' - TAGGTATCCCTACATCTGTAGT - 3' 3' - ATAGGGATGTAGACATCACAAA - 5'
Exon 3	5' - TAGGTGTTGGATGTGTGGTTAT - 3' 3' - ACAACCTACACACCAATACAAA - 5'

To measure intestinal cholesterol absorption, the fecal dual-isotope method was used on female *Oatp1a1*<sup>-/-</sup> *Ldlr*<sup>-/-</sup> mice (n = 7–8 per group; 8–17 weeks of age) that were injected with Bulevirtide for a total duration of 3 days. On the first day, mice received an oral bolus of radiolabeled cholesterol and reference marker sitostanol, after which mice were single-housed for the collection of feces. Fecal clearance of the radiolabels was measured in feces collected during the three days and bile salt levels were measured in feces collected during the final 24 h of the experiment. Three mice were excluded from all analyses based on liver pathology and strongly elevated plasma bile salt levels at baseline (n = 2 from the vehicle group and n = 1 from the Bulevirtide group).

### Plasma measurements

Bile salt levels were measured at the study endpoint in plasma. Total bile salt levels were measured using a Total Bile Acids Assay (DZ042A, Diazyme, Dresden, Germany) according to the manufacturer's protocol, and individual bile salt species were measured in 100  $\mu$ l plasma using high-performance liquid chromatography as described previously (6). Cholesterol and triglyceride concentration of very-low-density lipoproteins (VLDL), LDL, and high-density lipoproteins (HDL) isolated from plasma (50  $\mu$ l for cholesterol and 100  $\mu$ l for triglycerides per mouse) was determined using fast protein liquid chromatography (FPLC). The system contained a PU-980 ternary pump with an LG-980-02 linear degasser, FP-920 fluorescence, and UV-975 UV/VIS detectors (Jasco, Tokyo, Japan). An extra PU-2080i pump (Jasco, Tokyo Japan) was used for either in-line cholesterol PAP or Triglyceride enzymatic reagent (Roche, Basel, Switzerland) addition at a flow rate of 0.1 ml/minute. Plasma lipoproteins were separated using a Superose 6 Increase 10/30 column (GE Healthcare, Hoevelaken, The Netherlands) using Tris-buffered saline (pH 7.4), as eluent at a flow rate of 0.31 ml/minute. Commercially available lipid plasma standards (low, medium, and high) were used for the generation of total cholesterol or triglyceride calibration curves (SKML, Nijmegen, the Netherlands). Quantitative analysis of the chromatograms was carried out with Chrom Nav chromatographic software, version 2.0 (Jasco, Tokyo, Japan). Cholesterol and triglycerides in lipoprotein fractions, as well as individual bile salt species, could not be measured in the plasma of all mice given the large plasma volume required for these analyses.

### Atherosclerosis quantification

Hearts were excised, embedded in Tissue-tek O.C.T. compound on cryomold molds, and frozen in isopentanol, prior to cross-sectioning using a Leica CM 1950 cryostat at  $-25^{\circ}\text{C}$  (7  $\mu$ m sections). Cross sections were stained with Oil red O. Atherosclerotic lesion area of cross sections throughout the aortic root with a distance of 42  $\mu$ m, starting at the first appearance of aortic valves until the disappearance of aortic valves, were quantified with imaging software (ImageJ; National Institutes of Health, Bethesda, Maryland), from which the mean atherosclerotic lesion area was calculated. Histological images representative of mean atherosclerotic lesion area were selected for each group and displayed in [supplemental Fig. S1D](#) and [Fig. 2D](#). Several *Ldlr*<sup>-/-</sup> (n = 2 from the vehicle group and n = 1 from the Bulevirtide group) and *Oatp1a1*<sup>-/-</sup> *Ldlr*<sup>-/-</sup> mice (n = 1 from the vehicle group and n = 6 from the Bulevirtide group) were excluded due to damage during the cross-sectioning.

### Western blotting

To confirm *Oatp1a1* knockout for the generation of *Oatp1a1*<sup>-/-</sup> *Ldlr*<sup>-/-</sup> mice, frozen liver tissue was lysed and homogenized as described previously (15). Proteins were transferred by semi-dry blotting to PVDF membrane and probed with anti-rat OATP1A1 (1:1000, provided by Prof. Dr B. Stieger). Immune complexes were detected with a horseradish peroxidase-conjugated secondary antibody (Bio-Rad), visualized using enhanced chemiluminescence detection reagent (Lumi-light, Roche), and detected using ImageQuant LAS 4000 (GE Healthcare).

### Plasma clearance and biliary excretion of bile salts

After anesthesia, the gallbladder was cannulated and depleted of bile through bile collection after distal ligation of the common bile duct for a duration of 30 min. Simultaneously, a second and third cannula was inserted in the arteria carotis communis and vena jugularis for blood collection and bile salt infusion, respectively. After the 30 min bile depletion, 100  $\mu$ l 30 mM sodium taurocholic acid (TC) (T4009, Sigma-Aldrich, Saint Louis, Missouri, USA; dissolved in 0.9% NaCl) with 0.15  $\mu$ Ci [<sup>3</sup>H]TC (NET322, PerkinElmer) per mouse was infused via the vena jugularis, and blood and bile were sampled 2, 5, 10, 30, and 60 min post-infusion. Plasma (5  $\mu$ l) or bile (total collected volume) was directly added to 2.5 ml Ultima Gold. <sup>3</sup>H-activity was measured with a liquid scintillation counter (Tri-Carb 2900 TR, PerkinElmer) and expressed as a percentage of injected dose in plasma or bile. Bile flow was determined gravimetrically assuming a density of 1 g/ml for bile and expressed as  $\mu$ L per minute per 100 g of body weight.

### Flow cytometry

Blood was obtained by cardiac puncture and collected in tubes containing EDTA. Spleens were homogenized and filtered through a 70  $\mu$ m cell strainer (Corning). Blood and spleen were incubated with hypotonic lysis buffer (150 mM ammonium chloride, 10 mM sodium bicarbonate, 5 mM ethylenediaminetetraacetic acid (EDTA) (pH 7.4)) to remove erythrocytes. Samples were resuspended and stained in staining buffer (0.5% bovine serum albumin, 5 mM EDTA in PBS; pH 7.4). In the atherosclerosis study with *Ldlr*<sup>-/-</sup> mice, myeloid populations were identified using the following antibodies:  $\alpha$ CD45 (1:100, APC-Cy7, #103115, BioLegend, San Diego, California, USA),  $\alpha$ CD11b (1:200, BV711, #101241, BioLegend), F4/80 (1:100, #123108, BioLegend),  $\alpha$ Ly6C (1:100, AF647, #128010, BioLegend),  $\alpha$ Ly6G (1:800, FITC, #11-5931, Thermo Fisher Scientific, Waltham, Massachusetts, USA), and  $\alpha$ CD16/ $\alpha$ CD32 (1:1000, BioLegend, #101330). In the short-term study with *Oatp1a1*<sup>-/-</sup> *Ldlr*<sup>-/-</sup> mice, T cell populations were identified using the following antibodies:  $\alpha$ CD3 (1:200, APC-Cy7, #100222, BioLegend),  $\alpha$ CD4 (1:800, BV650, 100,469, BioLegend),  $\alpha$ CD8 (1:1000, BV605, #100744, BioLegend),  $\alpha$ CD44 (1:300, FITC, #103006, BioLegend),  $\alpha$ CD62L (1:1000, PE-Cy7, #104418, BioLegend), and  $\alpha$ CD16/ $\alpha$ CD32 (1:1000, #101330, BioLegend). Prior to analysis, 7-AAD was added (1:1000, #A1310, Thermo Fisher Scientific) to exclude dead cells. Cells were measured on a BD FACSymphony A1 Cell Analyzer (BD Biosciences) and data were analyzed using FCS Express software, version 7 (De Novo Software).

### Gene expression

RNA was isolated from frozen liver (approx. 50 mg) by lysis and homogenization using TRI Reagent (Invitrogen)

according to the manufacturer's protocols. One thousand ng of total RNA was treated with DNase (Promega, Leiden, The Netherlands), first-strand cDNA was synthesized with oligo-dT and SuperScript First-Strand Synthesis System (Invitrogen), and RT-qPCR was carried out in a QuantStudio 5 Real-Time (Thermo Fisher Scientific) using SYBR green reagent (Agilent Technologies) according to the manufacturer's protocols. Expression levels in each sample were normalized to the geometrical mean of glyceraldehyde-3-phosphate dehydrogenase (*Gapdh*) and hypoxanthine phosphoribosyltransferase (and expressed relative to the vehicle group using the  $2^{-\Delta\Delta CT}$  method. Primer sequences are provided in [supplemental Table S1](#).

### Intestinal cholesterol absorption and fecal lipid extraction

Intestinal cholesterol absorption was assessed using the fecal dual-isotope ratio method as described previously (16). In short, mice were subjected to an oral bolus of 100  $\mu$ l olive oil containing 1  $\mu$ Ci [ $^{14}$ C]cholesterol (ARC0857, American Radio-labeled) and 1  $\mu$ Ci [ $^3$ H]sitostanol (ART0361, American Radio-labeled Chemicals) and were subsequently single-housed for 3 days for feces collection. Fecal lipids were extracted using a protocol adapted from Srivastava (17) as follows. Feces were weighed, after which 50–70 mg was added to a tube containing ice-cold methanol (5  $\mu$ l per mg feces) and a steel bead, followed by lysis using a TissueLyser LT (50  $s^{-1}$  for 10 min; Qiagen). Samples were vortexed and sonicated for 45 min using an ice-filled Sonication bath 92 (Branson Ultrasonics). Subsequently, chloroform was added (methanol:chloroform ratio of 1:3), and samples were vortexed, transferred to glass tubes, and incubated at 4°C for 16 h. Next, samples were vortexed, sonicated for 45 min, and supplemented with PBS (methanol:PBS ratio of 1:2), prior to vortexing and centrifugation (4000 rpm, 30 min, 4°C). Two-thirds of the lipid-containing lower layer was transferred to a new glass tube, and heated under a stream of nitrogen (1 h, 42°C). Dried samples were dissolved in 500  $\mu$ l 2% Triton X-100 PBS solution, heated (1 h, 42°C), vortexed, and sonicated for 45 min.  $^{14}$ C- and  $^3$ H-activity was measured with a scintillation counter (Tri-Carb 2900TR, PerkinElmer, Waltham, Massachusetts, USA). Fecal [ $^{14}$ C]cholesterol content was normalized to the retrieved [ $^3$ H] activity and expressed cumulatively as a percentage of the inserted dosage. Intestinal [ $^{14}$ C]cholesterol uptake was calculated by subtracting the cumulative excretion from 100%.

### Fecal measurements

Lipids from feces were extracted as described above, in which total bile salt content was measured as described above. Values were normalized to the retrieved [ $^3$ H] activity and expressed as  $\mu$ mol per 24 h.

### Hepatic bile salt and cholesterol levels

Bile salts were extracted from the liver as follows. Liver tissue was weighed, after which 125–430 mg was added to a tube with 5 volumes of water and a steel bead, followed by lysis using a TissueLyser LT (50  $s^{-1}$  for 10 min; Qiagen). Subsequently, 1 ml acetonitrile was added to 200  $\mu$ l homogenate, followed by vortexing, incubation on ice for 10 min and centrifugation (14,000 rpm, 15 min, 4°C). Next, 1 ml supernatant was transferred to a new tube and was dried at 45°C using a 5301 concentrator (Eppendorf), following the addition of

250  $\mu$ l methanol (methanol:PBS ratio of 1:3). Bile salt composition in 100  $\mu$ l was analyzed by using high-performance liquid chromatography as described previously (6). Two mice were excluded from the analysis due to an insufficient amount of sample ( $n = 1$  from the vehicle group and  $n = 1$  from the Bulevirtide group). Lipids from liver tissue (50 mg per mouse) were extracted as described under 2.8, and total cholesterol content was measured using an enzymatic Cobas Total Cholesterol (106570) kit (Roche Diagnostics), by combining 7.5  $\mu$ l sample with 200  $\mu$ l reagent (the reagent was 3 $\times$  diluted) prior to incubation at room temperature for 30 min and measuring transmittance at 505 nm versus 650 nm.

### Statistical analyses

Statistical analyses between groups were performed with unpaired t-tests or Mann-Whitney U tests in case of non-normal distributions. Fecal [ $^{14}$ C]cholesterol excretion and [ $^3$ H]TC plasma clearance were analyzed by two-way analysis of variance (ANOVA) and following Šídák's multiple comparison post hoc test.  $P < 0.05$  was considered statistically significant. Significant outliers were identified with Grubbs' outlier test and removed from the analysis ( $\alpha = 5\%$ ). An overview of excluded outliers is displayed in [supplemental Table S2](#). Statistical analyses were performed with GraphPad Prism software, version 9.3.1 (GraphPad). Data are presented as individual data points and/or as means  $\pm$  SD.

## RESULTS

### NTCP inhibition by Bulevirtide treatment does not alter atherosclerosis lesion area in *Ldlr*<sup>-/-</sup> mice with intact *Oatp1a1*

*Ldlr*<sup>-/-</sup> mice were injected with Bulevirtide or vehicle daily for a total duration of 11 weeks. In line with our previous observation showing that OATP1A/1B family members have a substantially more predominant role in hepatic bile salt uptake in mice compared with humans (6), Bulevirtide treatment did not affect bile salt levels in plasma collected after 11 weeks of treatment ([supplemental Fig. S1A, B](#)), and body weight was unchanged ([supplemental Fig. S1C](#)). Correspondingly, Bulevirtide treatment did not alter the atherosclerotic lesion area ([supplemental Fig. S1D, E](#)) or cholesterol and triglyceride concentrations in VLDL, LDL, and HDL ([supplemental Fig. S1F, G](#)).

### NTCP inhibition by Bulevirtide treatment reduces atherosclerosis in *Oatp1a1*-deficient *Ldlr*<sup>-/-</sup> mice

Since the lack of induction of plasma bile salt levels upon Bulevirtide treatment is in contrast to observations in humans, we generated *Oatp1a1*<sup>-/-</sup> *Ldlr*<sup>-/-</sup> mice as a model with reduced contribution of OATPs to hepatic bile salt uptake, to more closely resemble hepatic bile salt uptake in humans ([Fig. 1A, B](#)). We assessed plasma clearance and biliary excretion of [ $^3$ H]TC in gallbladder-cannulated *Oatp1a1*<sup>-/-</sup> *Ldlr*<sup>-/-</sup> mice. Plasma clearance was indeed delayed compared with wild-type (group and time-group effect by two-way ANOVA:  $P = 0.0073$  and  $P < 0.001$ ), whereas biliary [ $^3$ H]TC excretion or total bile flow was not significantly altered

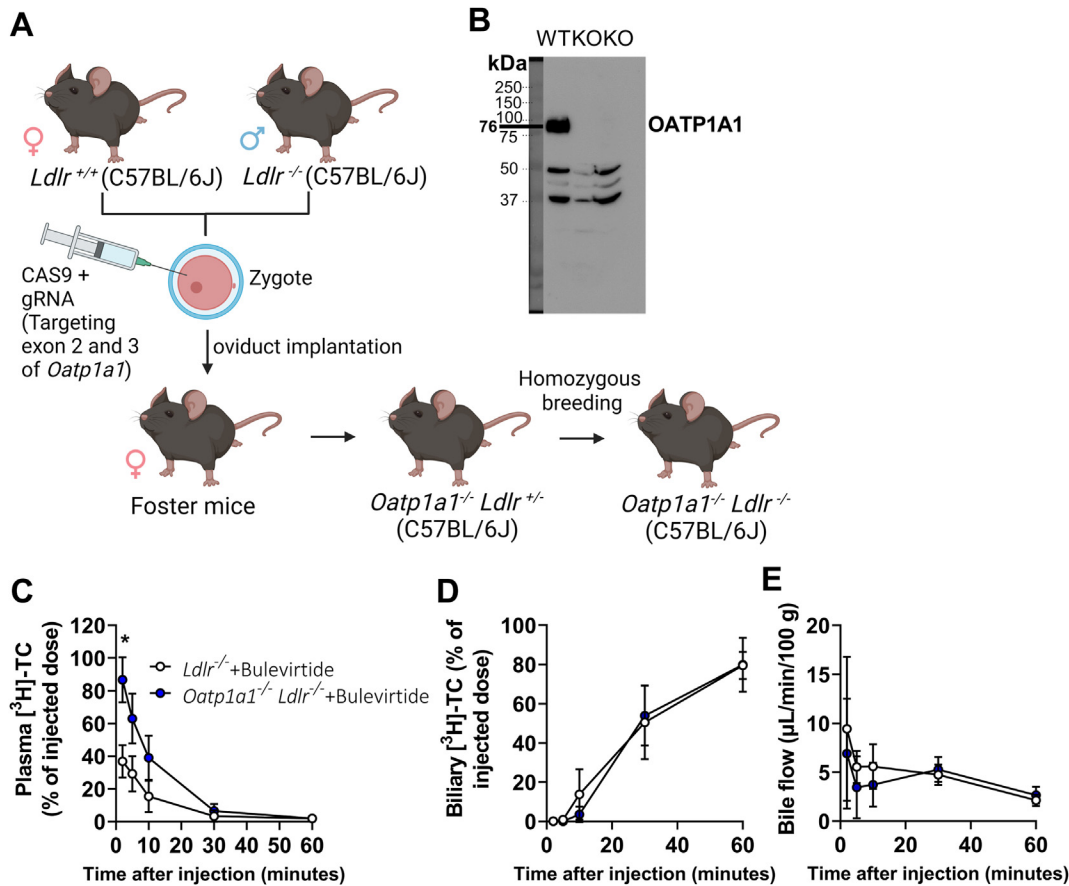


**Fig. 1.** Bulevirtide treatment delays clearance and increases levels of plasma bile salts in  $Oatp1a1^{-/-}$   $Ldlr^{-/-}$  mice. Using CRISPR/CAS9 the  $mOatp1a1$  locus was mutated in order to generate  $Oatp1a1^{-/-}$   $Ldlr^{-/-}$  mice. A: sgRNA was targeted to exon 2 and 3 of the  $mOatp1a1$  locus and together with Cas9 injected in the cytoplasm of a zygote derived from  $Ldlr^{+/+}$  and  $Ldlr^{-/-}$  mice, after which the zygote was implanted into the oviducts of foster mice. Breeding was continued to obtain homozygous  $Oatp1a1^{-/-}$   $Ldlr^{-/-}$  mice. B: Hepatic OATP1A1 abundance was measured in offspring to confirm knockout (KO) (third lane). The second lane served as a KO control. The gallbladder of male and female  $Oatp1a1^{-/-}$   $Ldlr^{-/-}$  (blue circle) or  $Oatp1a1^{+/+}$   $Ldlr^{-/-}$  mice (white circle) treated with a single dose of Bulevirtide was cannulated and [ $^3\text{H}$ ]sodium taurocholic acid (TC) was administered intravenously to measure [ $^3\text{H}$ ]-TC clearance from (C) plasma and (D) bile and to measure (E) bile flow, which was expressed as  $\mu\text{L}/\text{minute}/100\text{ g}$  body weight ( $n = 3\text{--}5/\text{group}$ ). Data are presented as means  $\pm$  SD. \*Vehicle versus Bulevirtide. \*  $P < 0.05$ , according to two-way ANOVA and following Sidák's multiple-comparisons test (C). Fig. 1A was created with BioRender.com.

(Fig. 1C–E). As there is a delay between excretion and sampling of bile due to the length of the gallbladder cannula, the unchanged biliary [ $^3\text{H}$ ]TC excretion is possibly caused by the sampling frequency. Corresponding to accelerated [ $^3\text{H}$ ]TC plasma clearance, Bulevirtide caused a modest though significant increase in systemic bile salt levels measured in another cohort after 10 weeks of treatment (Fig. 2A, B), without altering body weight (Fig. 2C). Despite the modest increase in plasma bile salt levels relative to humans, Bulevirtide reduced atherosclerotic lesion area in  $Oatp1a1^{-/-}$   $Ldlr^{-/-}$  mice (Fig. 2D, E).

#### NTCP inhibition by Bulevirtide treatment lowers plasma cholesterol levels in $Oatp1a1$ -deficient $Ldlr^{-/-}$ mice

To obtain insight in the mechanisms through which Bulevirtide attenuates atherosclerosis development, we measured the relative abundance of myeloid cells

(cluster of differentiation (CD)45<sup>+</sup> CD11b<sup>+</sup>Ly6G<sup>+</sup>) in blood and spleen of  $Oatp1a1^{-/-}$   $Ldlr^{-/-}$  mice collected at study endpoint (supplemental Fig. S2), since monocytes play an essential role in atherosclerosis development. Monocytes can be distinguished as non-classical (lymphocyte antigen 6 family member C (Ly6C)<sup>low</sup>), intermediate (Ly6C<sup>int</sup>), and classical (Ly6C<sup>hi</sup>) monocytes. However, Bulevirtide did not alter relative abundance in any of the subsets in blood (supplemental Fig. S2A–C) or spleen (supplemental Fig. S2D–F) after 10 weeks of treatment. We therefore continued with assessing cholesterol and triglyceride concentrations in VLDL, LDL, and HDL (Fig. 2F, G) that are tightly linked to atherosclerosis development. In line with reduced atherosclerotic lesion area (Fig. 2D, E), Bulevirtide reduced cholesterol concentrations, which were confined to LDL (–11.3%) and HDL (–20.0%) (Fig. 2F), while triglyceride concentrations were unchanged (Fig. 2G). Interestingly, Bulevirtide treatment lowered

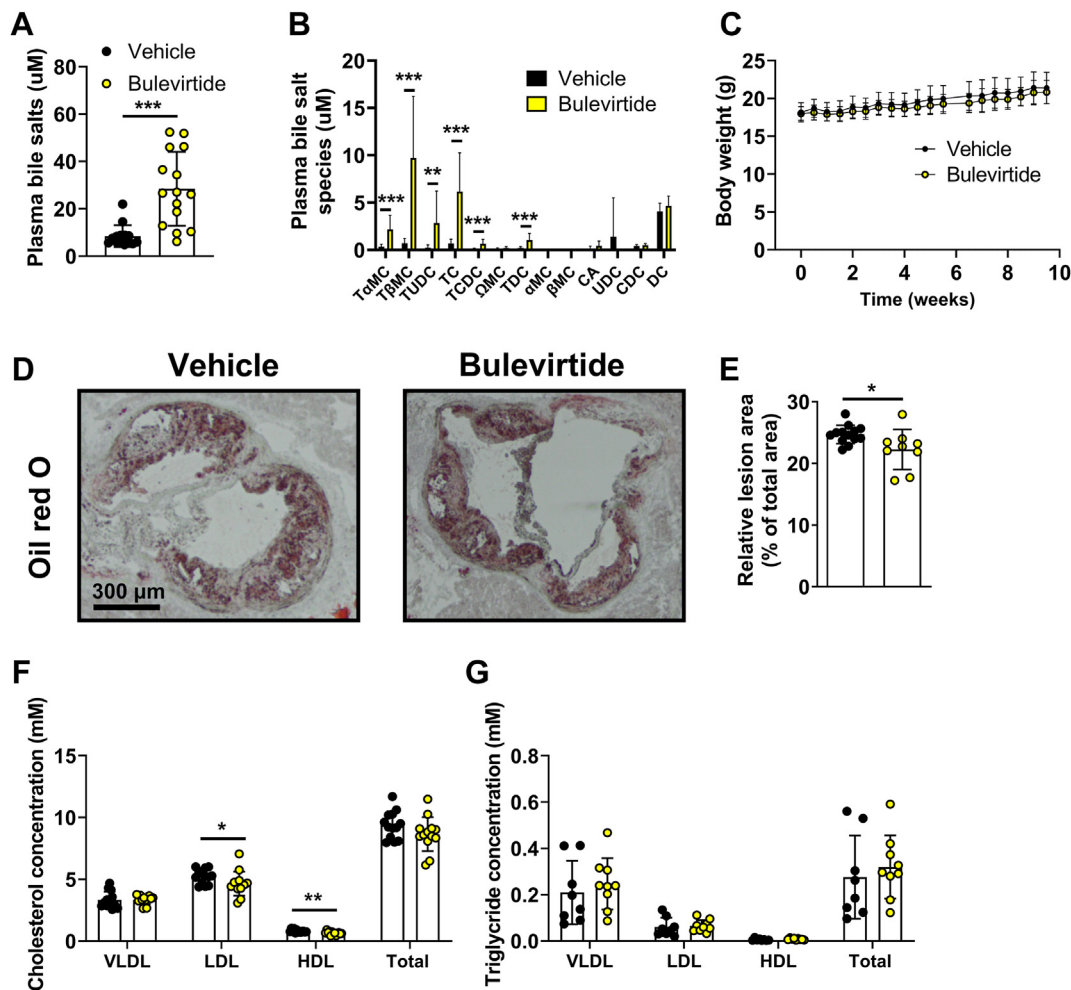


**Fig. 2.** Bulevirtide treatment attenuates atherosclerosis development and lowers plasma cholesterol levels in *Oatp1a1*<sup>-/-</sup> *Ldlr*<sup>-/-</sup> mice. Female *Oatp1a1*<sup>-/-</sup> *Ldlr*<sup>-/-</sup> mice were injected subcutaneously with Na<sup>+</sup> taurocholate co-transporting polypeptide (NTCP) inhibitor Bulevirtide (yellow circles or bars) or vehicle (black circles or bars) every day for 10 weeks. At study endpoint, (A) total plasma bile salt levels and (B) individual bile salt species were measured, including tauro- $\alpha$ -muricholic acid (T $\alpha$ MC), tauro- $\beta$ -muricholic acid (T $\beta$ MC), tauroursodeoxycholic acid (TUDC), taurocholic acid (TC), taurochenodeoxycholic acid (TCDC), omega-muricholic acid ( $\Omega$ MC), taurodeoxycholic acid (TDC),  $\alpha$ -muricholic acid ( $\alpha$ MC),  $\beta$ -muricholic acid ( $\beta$ MC), cholic acid (CA), ursodeoxycholic acid (UDC), chenodeoxycholic acid (CDC), and deoxycholic acid (DC) (n = 14–15/group). C: Body weight was monitored throughout the study (n = 15–16/group). Cross-sections of the aortic root area were stained with Oil red O to visualize atherosclerotic lesions from which the area was determined. D: Representative images of each staining are displayed and (E) mean atherosclerotic lesion area was expressed relative to the total area of the aortic root (n = 9–14/group). Plasma (F) cholesterol (n = 13/group) and (G) triglyceride concentration (n = 8–9/group) was measured in very-low-density lipoprotein (VLDL), low-density lipoprotein (LDL), and high-density lipoprotein (HDL). Data are presented as means  $\pm$  SD. \*Vehicle versus Bulevirtide. \* *P* < 0.05, according to Mann Whitney's test (A), or student's *t* test (B, E, F).

hepatic expression of farnesoid X receptor (*Nr1h4*) and its target gene organic solute transporter beta (*Slc51b*), but not fatty acid synthetase (*Fasn*), small heterodimer partner (*Nr0b2*), or pregnane X receptor (*Nr1i2*) (Fig. 3A–E). However, expression of cytochrome P450 family 7 subfamily A member 1 (*Cyp7a1*), cytochrome P450 family 27 subfamily A member 1 (*Cyp27a1*), and cytochrome P450 family 8 subfamily B member 1 (*Cyp8b1*) was unchanged (Fig. 3F–H), suggesting unaltered hepatic bile salt synthesis at the time point the tissues were collected, 6 h into the light phase. Bulevirtide treatment did not affect genes involved in cholesterol metabolism, including apolipoprotein A1

(*Apoa1*), apolipoprotein B (*Apob*), apolipoprotein C2 (*Apoc2*), ATP binding cassette subfamily A member 1 (*Abca1*), LDL receptor-related protein 1 (*Lrp1*), 3-hydroxy-3-methyl-glutaryl-coenzyme A reductase (*Hmgcr*), ATP-binding cassette sub-family G member 5 (*Abcg5*), and ATP-binding cassette sub-family G member 8 (*Abcg8*) (Fig. 3I–P).

In a follow-up experiment, we treated *Oatp1a1*<sup>-/-</sup> *Ldlr*<sup>-/-</sup> mice with Bulevirtide for 3 days to closely study the immune system and to elucidate the mechanisms underlying the reduction in plasma cholesterol levels. We confirmed that Bulevirtide treatment increased plasma bile salt levels (Fig. 4A). First, we investigated

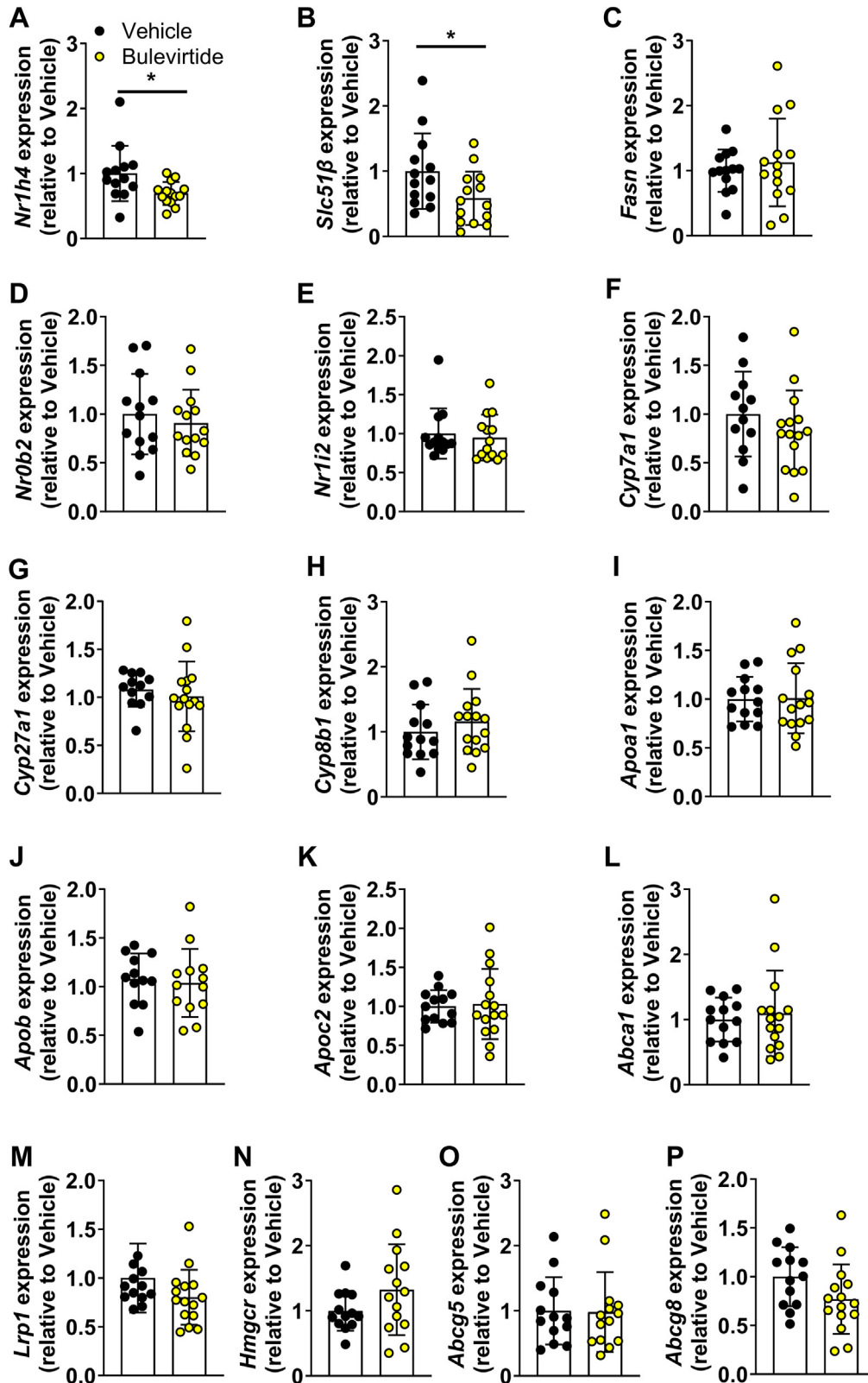


**Fig. 3.** Bulevirtide treatment does not alter hepatic expression of genes involved in bile salt or cholesterol metabolism in *Oatp1a1*<sup>-/-</sup> *Ldlr*<sup>-/-</sup> mice. Female *Oatp1a1*<sup>-/-</sup> *Ldlr*<sup>-/-</sup> mice were injected subcutaneously with Na<sup>+</sup> taurocholate co-transporting polypeptide (NTCP) inhibitor Bulevirtide (yellow circles or bars) or vehicle (black circles or bars) every day for 10 weeks. Hepatic gene expression of (A) farnesoid X receptor (*Nr1h4*), (B) organic solute transporter beta (*Slc51β*), (C) fatty acid synthetase (*Fasn*), (D) small heterodimer partner (*Nr0b2*), (E) pregnane X receptor (*Nr1i2*), (F) cytochrome P450 family 7 subfamily A member 1 (*Cyp7a1*), (G) cytochrome P450 family 27 subfamily A member 1 (*Cyp27a1*), (H) cytochrome P450 family 8 subfamily B member 1 (*Cyp8b1*), (I) apolipoprotein A1 (*Apoa1*), (J) apolipoprotein B (*Apob*), (K) apolipoprotein C2 (*Apoc2*), (L) ATP binding cassette subfamily A member 1 (*Abca1*), (M) LDL receptor related protein 1 (*Lrp1*), (N) 3-hydroxy-3-methyl-glutaryl-coenzyme A reductase (*Hmgcr*), (O) ATP-binding cassette sub-

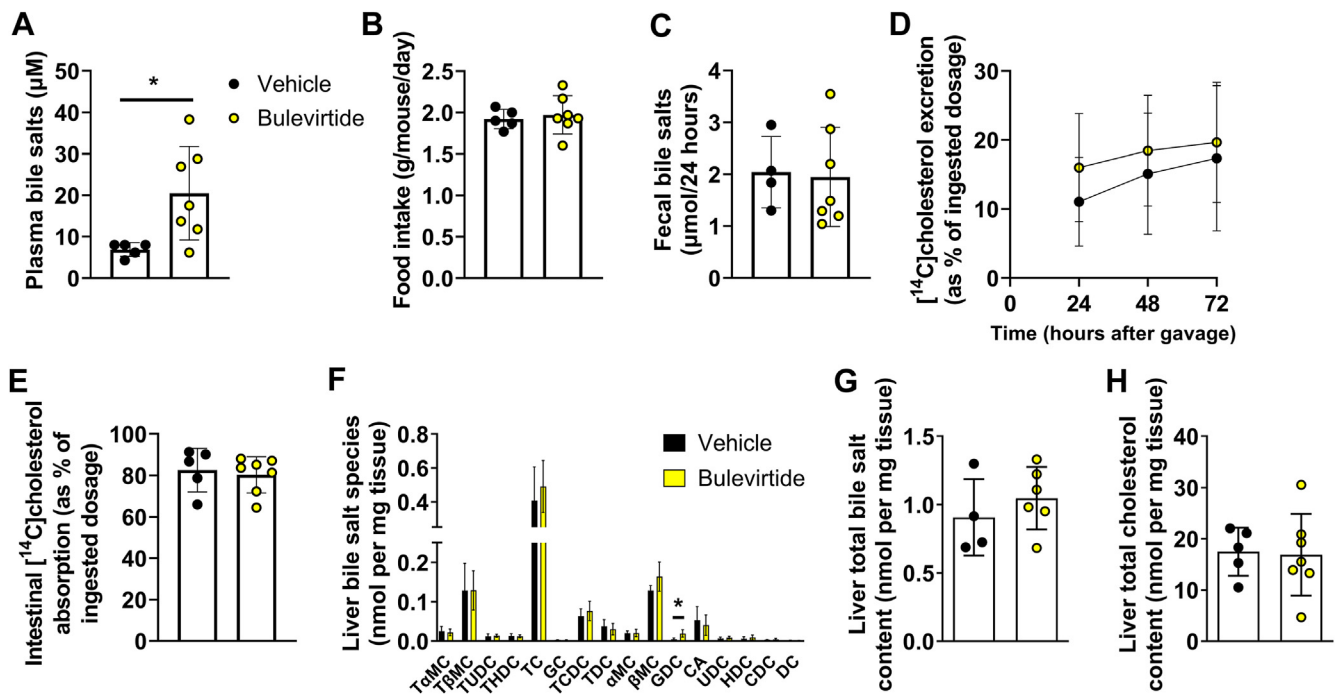


**Fig. 4.** Bulevirtide treatment does not alter food intake, fecal bile salt levels, or intestinal cholesterol absorption in *Oatp1a1<sup>-/-</sup> Ldlr<sup>-/-</sup>* mice. Female *Oatp1a1<sup>-/-</sup> Ldlr<sup>-/-</sup>* mice were injected subcutaneously with Na<sup>+</sup> taurocholate co-transporting polypeptide (NTCP) inhibitor Bulevirtide (yellow circles) or vehicle (black circles) every day for 3 days after administration of an oral bolus of [<sup>14</sup>C]cholesterol and [<sup>3</sup>H]sitostanol in olive oil. A: Plasma bile salts were measured after 3 days and (B) food intake was monitored throughout the 3 days (C) Bile salt levels were measured in feces collected during the last 24 h of treatment. <sup>3</sup>H and <sup>14</sup>C activity were determined in feces samples after 24, 48, and 72 h after administration of the tracers from which (D) fecal [<sup>14</sup>C]cholesterol excretion and (E) intestinal uptake were calculated. F: In the liver individual bile salt species were measured, including tauro- $\alpha$ -muricholic acid (T $\alpha$ MC), tauro- $\beta$ -muricholic acid (T $\beta$ MC), tauroursodeoxycholic acid (TUDC), taurohyodeoxycholic acid (THDC), taurocholic acid (TC), glycocholic acid (GC), taurochenodeoxycholic acid (TCDC), taurodeoxycholic acid (TDC),  $\alpha$ -muricholic acid ( $\alpha$ MC),  $\beta$ -muricholic acid ( $\beta$ MC), glycodeoxycholic acid (GDC), cholic acid (CA), ursodeoxycholic acid (UDC), hyodeoxycholic acid (HDC), chenodeoxycholic acid (CDC), and deoxycholic acid (DC). G: Total bile salt content was calculated by adding individual species. H: Hepatic total cholesterol content was measured. Data are presented as means  $\pm$  SD (n = 4–7/group). \*Vehicle versus Bulevirtide. \* *P* < 0.05, according to student's *t* test (A) or two-way ANOVA (D).

the immune system more closely by measuring the relative abundance of T cell populations in the blood and spleen of the mice in this follow-up experiment. However, Bulevirtide did not alter the abundance of the T cell populations (supplemental Fig. S3). Next, we explored cholesterol metabolism and started by assessing food intake to test whether Bulevirtide treatment lowers plasma cholesterol levels by altering dietary cholesterol intake, which was not the case (Fig. 4B). Since we previously observed that genetic deletion of NTCP lowers intestinal lipid absorption (5), we hypothesized that Bulevirtide interferes with intestinal cholesterol absorption through impaired emulsification of dietary cholesterol by altering intestinal bile salt levels. To this end, we subjected mice to an oral bolus of [<sup>14</sup>C]cholesterol and [<sup>3</sup>H]sitostanol as a non-absorbable reference marker, and measured fecal secretion of the radiolabels for a duration of 72 h, from which fecal cholesterol excretion and intestinal cholesterol

absorption were calculated. However, Bulevirtide treatment did not alter fecal bile salt levels (Fig. 4C), and while the fecal [<sup>14</sup>C]cholesterol excretion rate, reflecting unabsorbed cholesterol from the oral bolus, appeared to be higher in the Bulevirtide-treated mice (time-group interaction by two-way ANOVA: *P* = 0.045), intestinal [<sup>14</sup>C]cholesterol absorption after 72 h was not significantly reduced (Fig. 4D, E). In line with the unchanged hepatic expression of genes involved in bile salt and cholesterol metabolism after 10 weeks of Bulevirtide treatment (Fig. 3), hepatic bile salt and cholesterol levels were mostly unchanged after 3 days of treatment (Fig. 4F–H).

## DISCUSSION

Bile salts exert beneficial effects on metabolic health by acting as strong signaling hormones, but agonists targeting the bile salt receptor FXR elevate plasma

family G member 5 (*Abcg5*), and (P) ATP-binding cassette sub-family G member 8 (*Abcg8*) was determined by quantitative polymerase chain reaction, normalized to glyceraldehyde-3-phosphate dehydrogenase (*Gapdh*) and hypoxanthine phosphoribosyltransferase (*Hprt*) and shown relative to the expression in the vehicle group (n = 13–15/group). Data are presented as means  $\pm$  SD.



cholesterol levels and thereby potentially elevate asCVD risk. In contrast, we here show that NTCP inhibition by Bulevirtide treatment lowers plasma cholesterol levels and modestly reduces atherosclerosis lesion area in *Oatp1a1*<sup>-/-</sup> *Ldlr*<sup>-/-</sup> mice, a hyperlipidemic and atherosclerosis-prone mouse model that more closely resembles human hepatic bile salt uptake than mice with intact OATPs.

Bile salts have many potential beneficial effects on atherosclerosis development. Several preclinical studies have shown that agonists of the bile salt receptors TGR5 and FXR attenuate atherosclerosis development in rodent models (18–21). The anti-atherogenic properties of FXR agonists could likely be attributed to an improved lipoprotein profile due to enhanced hepatic cholesterol excretion and reduced intestinal cholesterol absorption (18, 19). In our study, Bulevirtide treatment did not alter intestinal cholesterol absorption, although detecting subtle differences in mechanisms underlying the small but significant plasma LDL-c reduction might be difficult. Nonetheless, we previously demonstrated that Bulevirtide increases biliary cholesterol excretion independent of the cholesterol transporters *Abcg5* and *Abcg8*, by shifting hepatic bile salt uptake from mainly periportal hepatocytes towards pericentral hepatocytes, thereby increasing exposure of the canalicular membrane to bile salts (22). Future studies should further elucidate potential mechanisms underlying changes in lipoprotein metabolism upon NTCP inhibition. In contrast to FXR agonists, the TGR5 agonist 6 $\alpha$ -ethyl-23(S)-methylcholic acid was shown to attenuate atherosclerosis development through its anti-inflammatory properties that seem to be dependent on monocytes and T cells (20). In contrast, Bulevirtide treatment in our study did not affect monocyte or T cell populations, suggesting that the anti-atherogenic effects were cholesterol-driven. A likely reason for the discrepancy in effects between the administration of synthetic FXR or TGR5 agonists and NTCP inhibition is that the latter increases plasma levels of endogenous bile salts in a meal-dependent fashion, as opposed to strong receptor activation. In addition, this mixture of bile salts has varying binding capacity to FXR and TGR5 and could also bind to yet-unidentified bile salt receptors.

TGR5 and FXR agonists have limited therapeutic potential for asCVD since studies as TGR5 agonists were not pursued into clinical trials due to side effects in animal models and the FXR agonist obeticholic acid (OCA) increases LDL-c and lowers HDL-c in patients (23). On the contrary, ASBT inhibitors are more promising candidates to reach the clinic for the treatment of asCVD as they were shown to reduce plasma LDL-c levels in humans (24–26), which translated to a reduction in atherosclerosis development in animal models (27). Mechanistically, ASBT inhibition lowers plasma cholesterol levels by inducing cholesterol turnover through stimulating hepatic bile salt synthesis

(27–29). In our study, gene expression analysis did not indicate alterations in hepatic bile salt synthesis upon Bulevirtide treatment, suggesting different cholesterol-reducing pathways between ASBT and NTCP inhibition, although temporally-restricted effects on FXR agonism may be present, as expression of the sensitive FXR-target gene *Slc51 $\beta$*  was significantly dampened.


In our study, Bulevirtide treatment did not attenuate atherosclerosis development or lower plasma cholesterol levels in *Ldlr*<sup>-/-</sup> mice with intact *Oatp1a1*, which could likely be attributed to the insufficient inhibition of hepatic bile salt uptake. Genetic deletion of *Oatp1a1* appeared to be sufficient to lower hepatic bile salt uptake capacity and to elicit an average increase in plasma bile salt levels to 20–30  $\mu$ M upon Bulevirtide treatment, and correspondingly reduced atherosclerosis lesion area, albeit modestly. In humans, Bulevirtide injections increase average plasma bile salt levels up to 200  $\mu$ M (8, 30). We therefore anticipate that the cholesterol-lowering effects of Bulevirtide might be more pronounced in humans. Indeed, in our study Bulevirtide treatment lowered plasma cholesterol concentration in LDL and HDL fractions without altering total cholesterol levels, while in humans a genetic loss-of-function variant of NTCP in humans has been associated with reduced plasma LDL-c and total cholesterol levels without reductions in HDL-c (12). Similarly, in a recent phase I exploratory study Bulevirtide reduced plasma lipoprotein (a), increased plasma HDL-c, and lowered plasma LDL-c levels, changes that are associated with reduced asCVD risk (13). However, the LDL-c reduction was non-significant as the study was underpowered. Nonetheless, the mild LDL-c reduction in our study translates to a modest reduction in the atherosclerotic lesion area.

A translational limitation of our study is that Bulevirtide only mildly increased plasma bile salt levels compared with humans, indicating that genetic deletion of the OATP1A1 isoform is insufficient to humanize hepatic bile salt uptake. Furthermore, we solely utilized female mice for the atherosclerosis experiments. We have, however, previously demonstrated the beneficial metabolic effects of NTCP inhibition in both male and female mice (5, 11), suggesting that the anti-atherogenic effects also translate to male mice, which should be confirmed by future studies. Studies in humans on a genetic loss-of-function variant of NTCP and a phase I exploratory study on Bulevirtide included both men and women, suggesting that NTCP inhibition in humans lowers plasma cholesterol levels in both sexes (12, 13).

In conclusion, the NTCP inhibitor Bulevirtide reduces atherosclerotic lesion area likely by lowering plasma LDL-c levels. Bulevirtide administration is considered safe and has been EMA-approved for the treatment of Hepatitis D. We anticipate that its application may extend to cardiometabolic diseases, among which asCVD, which warrants validation in clinical

trials. Currently, ASBT inhibitors also pose as potential candidates for asCVD treatment. In recent trials on patients with MASLD/MASH (NCT04006145) or diabetes (31), the ASBT inhibitor elobixibat lowered plasma LDL-c levels but failed to improve other key MASH measures. Bulevirtide on the other hand might treat a wider range of cardiometabolic diseases, as we previously demonstrated in preclinical studies that NTCP inhibition protects against obesity, hepatosteatosis, and cholestasis (5, 10), in addition to atherosclerosis. Importantly, the development of oral NTCP inhibitors is required for the feasible application of this drug. Interestingly, dual ASBT/NTCP inhibitors are currently under development and may combine the beneficial cholesterol-reducing properties of both inhibitors (32).

### Data availability

The data that support the findings of this study are available from the corresponding author upon request. 

### Supplemental data

This article contains [supplemental data](#).

### Author contributions

B. P., R. R. A., W. I. H. P., R. P. J. O. F., E. L., and S. F. J. V. D. G. conceptualization; B. P., R. R. A., W. I. H. P., D. R. D. W., S. D., I. B., E. W. V., J. H. M. L., L. A. B., and W. G. V. investigation; B. P., R. R. A., and W. I. H. P. formal analysis; S. F. J. V. D. G.: funding acquisition; S. F. J. V. D. G.: supervision. B. P., R. R. A., W. I. H. P., R. P. J. O. F., E. L., S. F. J. V. D. G., D. R. D. W., S. D., I. B., E. W. V., J. H. M. L., L. A. B., and W. G. V. writing—original draft; B. P., R. R. A., W. I. H. P., R. P. J. O. F., E. L., S. F. J. V. D. G., D. R. D. W., S. D., I. B., E. W. V., J. H. M. L., L. A. B., and W. G. V. writing—review and editing.

### Author ORCIDi

Wietse In het Panhuis  <https://orcid.org/0000-0002-4394-6387>

Laura A. Bosmans  <https://orcid.org/0000-0002-1984-9691>

Winnie G. Vos  <https://orcid.org/0000-0001-7805-7275>

Stan F.J. van de Graaf  <https://orcid.org/0000-0003-4238-4359>

### Funding and additional information

Stan F. J. van de Graaf was supported by grants from the Netherlands Organization for Scientific Research (Vidi 91713319 and Vici 09150182010007 to SFJVDG) and the European Research Council (Starting grant no. 337479).

### Conflict of interest

The authors declare that they have no conflicts of interest with the contents of this article.

### Abbreviations

ABCG5, ATP-binding cassette sub-family G member 5; ABCG8, ATP-binding cassette sub-family G member 8; ApoA1, apolipoprotein A1; ApoB, apolipoprotein B; ApoC2,

apolipoprotein C2; ASBT, apical sodium dependent bile acid transporter; asCVD, atherosclerotic cardiovascular disease; CA, cholic acid; CD, cluster of differentiation; CDC, chenodeoxycholic acid; CYP7A1, cytochrome P450 family 7 sub-family A member 1; CYP27A1, cytochrome P450 family 27 subfamily A member 1; CYP8B1, cytochrome P450 family 8 subfamily B member 1; DC, deoxycholic acid; FASN, fatty acid synthetase; GC, glycocholic acid; GDC, glycodeoxycholic acid; HDC, hyodeoxycholic acid; HMGCR, 3-hydroxy-3-methyl-glutaryl-coenzyme A reductase; HPRT, hypoxanthine phosphoribosyltransferase; LRP1, LDL receptor related protein 1; Ly6C, (ymphocyte antigen 6 family member C; Nrlh4, farnesoid x receptor; Nrlh2, pregnane x receptor; NTCP, Na<sup>+</sup> taurocholate cotransporting polypeptide; OATP, organic anion transporting polypeptides; OCA, obeticholic acid; *Slc51β*, organic solute transporter beta; TαMC, tauro-alpha-muricholic acid; TβMC, tauro-beta-muricholic acid; TGR5, membrane-bound G protein-coupled bile acid receptor; TC, taurocholic acid; TCDC, taurochenodeoxycholic acid; TDC, taurodeoxycholic acid; THDC, aurohyodeoxycholic acid; TUDC, taurooursodeoxycholic acid; UDC, ursodeoxycholic acid; ZT, *Zeitgeber* Time; αMC, alpha-muricholic acid; βMC, beta-muricholic acid; ΩMC, omega-muricholic acid.

Manuscript received November 10, 2023, and in revised form June 5, 2024. Published, JLR Papers in Press, July 14, 2024, <https://doi.org/10.1016/j.jlr.2024.100594>

## REFERENCES

1. Kunst, R. F., Verkade, H. J., Elferink, R. P. O., and van de Graaf, S. F. (2021) Targeting the four pillars of enterohepatic bile salt cycling; lessons from genetics and pharmacology. *Hepatology*. **73**, 2577–2585
2. Donkers, J. M., Abbing, R. L. R., and Van de Graaf, S. F. (2019) Developments in bile salt based therapies: a critical overview. *Biochem. Pharmacol.* **161**, 1–13
3. Lavoie, B., Balemba, O. B., Godfrey, C., Watson, C. A., Vassileva, G., Corvera, C. U., *et al.* (2010) Hydrophobic bile salts inhibit gallbladder smooth muscle function via stimulation of GPBAR1 receptors and activation of KATP channels. *J. Physiol.* **588**, 3295–3305
4. Li, T., Holmstrom, S. R., Kir, S., Umetani, M., Schmidt, D. R., Kliever, S. A., *et al.* (2011) The G protein-coupled bile acid receptor, TGR5, stimulates gallbladder filling. *Mol. Endocrinol.* **25**, 1066–1071
5. Donkers, J. M., Kooijman, S., Slijepcevic, D., Kunst, R. F., Abbing, R. L. R., Haazen, L., *et al.* (2019) NTCP deficiency in mice protects against obesity and hepatosteatosis. *JCI Insight* **4**, e127197
6. Slijepcevic, D., Roscam Abbing, R. L., Katafuchi, T., Blank, A., Donkers, J. M., van Hoppe, S., *et al.* (2017) Hepatic uptake of conjugated bile acids is mediated by both sodium taurocholate cotransporting polypeptide and organic anion transporting polypeptides and modulated by intestinal sensing of plasma bile acid levels in mice. *Hepatology*. **66**, 1631–1643
7. Mak, L-Y, Cheung, K-S, Fung, J., Seto, W-K., and Yuen, M-F. (2022) New strategies for the treatment of chronic hepatitis B. *Trends Mol. Med.* **28**, P742–P757
8. Blank, A., Markert, C., Hohmann, N., Carls, A., Mikus, G., Lehr, T., *et al.* (2016) First-in-human application of the novel hepatitis B and hepatitis D virus entry inhibitor myrcludex B. *J. Hepatol.* **65**, 483–489
9. Wedemeyer, H., Aleman, S., Brunetto, M. R., Blank, A., Andreone, P., Bogomolov, P., *et al.* (2023) A phase 3, randomized trial of bulevirtide in chronic hepatitis D. *New Engl. J. Med.* **389**, 22–32
10. Slijepcevic, D., Roscam Abbing, R. L., Fuchs, C. D., Haazen, L. C., Beuers, U., Trauner, M., *et al.* (2018) Na<sup>+</sup>-taurocholate

- cotransporting polypeptide inhibition has hepatoprotective effects in cholestasis in mice. *Hepatology*. **68**, 1057–1069
11. Donkers, J. M., Abbing, R. L. R., van Weeghel, M., Levels, J. H., Boelen, A., Schinkel, A. H., *et al.* (2020) Inhibition of hepatic bile acid uptake by myrcludex B promotes glucagon-like peptide-1 release and reduces obesity. *Cell Mol. Gastroenterol. Hepatol.* **10**, 451–466
  12. Cheng, X., Wang, Y., Tian, J., Zhou, L., Chen, X., Guo, H., *et al.* (2019) SLC10A1 S267F variant influences susceptibility to HBV infection and reduces cholesterol level by impairing bile acid uptake. *J. Viral Hepat.* **26**, 1178–1185
  13. Stoll, F., Seidel-Glätzer, A., Burghaus, I., Göring, O., Sauter, M., Rose, P., *et al.* (2022) Metabolic effect of blocking sodium-taurocholate Co-transporting polypeptide in hypercholesterolemic humans with a twelve-week course of bulevirtide—an exploratory phase I clinical trial. *Int. J. Mol. Sci.* **23**, 15924
  14. Oppi, S., Lüscher, T. F., and Stein, S. (2019) Mouse models for atherosclerosis research—which is my line? *Front. Cardiovasc. Med.* **46**, 46
  15. Man, J. J., Beckman, J. A., and Jaffe, I. Z. (2020) Sex as a biological variable in atherosclerosis. *Circ. Res.* **126**, 1297–1319
  16. Wang, D. Q., and Carey, M. C. (2003) Measurement of intestinal cholesterol absorption by plasma and fecal dual-isotope ratio, mass balance, and lymph fistula methods in the mouse: an analysis of direct versus indirect methodologies. *J. Lipid Res.* **44**, 1042–1059
  17. Kumar Srivastava, N., Pradhan, S., Mittal, B., Kumar, R., and Nagana Gowda, G. (2006) An improved, single step standardized method of lipid extraction from human skeletal muscle tissue. *Anal. Lett.* **39**, 297–315
  18. Hartman, H. B., Gardell, S. J., Petucci, C. J., Wang, S., Krueger, J. A., and Evans, M. J. (2009) Activation of farnesoid X receptor prevents atherosclerotic lesion formation in LDLR<sup>-/-</sup> and apoE<sup>-/-</sup> mice. *J. Lipid Res.* **50**, 1090–1100
  19. Hambruch, E., Miyazaki-Anzai, S., Hahn, U., Matysik, S., Boettcher, A., Perović-Ottstadt, S., *et al.* (2012) Synthetic farnesoid X receptor agonists induce high-density lipoprotein-mediated transhepatic cholesterol efflux in mice and monkeys and prevent atherosclerosis in cholesteryl ester transfer protein transgenic low-density lipoprotein receptor (–/–) mice. *J. Pharmacol. Exp. Ther.* **343**, 556–567
  20. Pols, T. W., Nomura, M., Harach, T., Sasso, G. L., Oosterveer, M. H., Thomas, C., *et al.* (2011) TGR5 activation inhibits atherosclerosis by reducing macrophage inflammation and lipid loading. *Cell Metab.* **14**, 747–757
  21. Miyazaki-Anzai, S., Masuda, M., Levi, M., Keenan, A. L., and Miyazaki, M. (2014) Dual activation of the bile acid nuclear receptor FXR and G-protein-coupled receptor TGR5 protects mice against atherosclerosis. *PLoS One*. **9**, e108270
  22. Roscam Abbing, R. L., Slijepcevic, D., Donkers, J. M., Havinga, R., Duijst, S., Paulusma, C. C., *et al.* (2020) Blocking sodium-taurocholate cotransporting polypeptide stimulates biliary cholesterol and phospholipid secretion in mice. *Hepatology*. **71**, 247–258
  23. Mudaliar, S., Henry, R. R., Sanyal, A. J., Morrow, L., Marschall, H. U., Kipnes, M., *et al.* (2013) Efficacy and safety of the farnesoid X receptor agonist obeticholic acid in patients with type 2 diabetes and nonalcoholic fatty liver disease. *Gastroenterology*. **145**, 574–582.e1
  24. Palmer, M., Jennings, L., Silberg, D. G., Bliss, C., and Martin, P. (2018) A randomised, double-blind, placebo-controlled phase 1 study of the safety, tolerability and pharmacodynamics of volixibat in overweight and obese but otherwise healthy adults: implications for treatment of non-alcoholic steatohepatitis. *BMC Pharmacol. Toxicol.* **19**, 10
  25. Tiessen, R. G., Kennedy, C. A., Keller, B. T., Levin, N., Acevedo, L., Gedulin, B., *et al.* (2018) Safety, tolerability and pharmacodynamics of apical sodium-dependent bile acid transporter inhibition with volixibat in healthy adults and patients with type 2 diabetes mellitus: a randomised placebo-controlled trial. *BMC Gastroenterol.* **18**, 3
  26. Kumagai, Y., Amano, H., Sasaki, Y., Nakagawa, C., Maeda, M., Oikawa, I., *et al.* (2018) Effect of single and multiple doses of elobixibat, an ileal bile acid transporter inhibitor, on chronic constipation: a randomized controlled trial. *Br. J. Clin. Pharmacol.* **84**, 2393–2404
  27. West, K. L., Zern, T. L., Butteiger, D. N., Keller, B. T., and Fernandez, M. L. (2003) SC-435, an ileal apical sodium co-dependent bile acid transporter (ASBT) inhibitor lowers plasma cholesterol and reduces atherosclerosis in Guinea pigs. *Atherosclerosis*. **171**, 201–210
  28. Rao, A., Kusters, A., Mells, J. E., Zhang, W., Setchell, K. D., Amanso, A. M., *et al.* (2016) Inhibition of ileal bile acid uptake protects against nonalcoholic fatty liver disease in high-fat diet-fed mice. *Sci. Transl. Med.* **8**, 357ra122
  29. Lan, T., Haywood, J., and Dawson, P. A. (2013) Inhibition of ileal apical but not basolateral bile acid transport reduces atherosclerosis in apoE<sup>-/-</sup> mice. *Atherosclerosis*. **229**, 374–380
  30. Haag, M., Hofmann, U., Mürdter, T. E., Heinkele, G., Leuthold, P., Blank, A., *et al.* (2015) Quantitative bile acid profiling by liquid chromatography quadrupole time-of-flight mass spectrometry: monitoring hepatitis B therapy by a novel Na<sup>+</sup>-taurocholate cotransporting polypeptide inhibitor. *Anal. Bioanal. Chem.* **407**, 6815–6825
  31. Yoshinobu, S., Hasuzawa, N., Nagayama, A., Iwata, S., Yasuda, J., Tokubuchi, R., *et al.* (2022) Effects of elobixibat, an inhibitor of ileal bile acid transporter, on glucose and lipid metabolism: a single-arm pilot study in patients with t2dm. *Clin. Ther.* **44**, 1418–1426
  32. Strängberg, E., Gillberg, P-G., Uzelac, I., Starke, I., Bonn, B., Mattsson, J., *et al.* (2022) Dual ileal/renal-liver bile acid transporter inhibitors with different transporter selectivity in vitro differentially increase faecal and urinary bile acid excretion in organic anion transporting polypeptide 1a/1b knockout mice in vivo. *J. Hepatol.* **77**, S751–S752